

Measurement of Aharonov-Bohm oscillations in mesoscopic metallic rings in the presence of a high-frequency electromagnetic field

Josef-Stefan Wenzler and Pritiraj Mohanty

Department of Physics, Boston University, 590 Commonwealth Avenue, Boston, Massachusetts 02215, USA

(Received 25 February 2008; published 31 March 2008)

We report measurements of Aharonov-Bohm oscillations in normal metal rings in the presence of high-frequency electromagnetic fields. The power dependence of the decoherence time scale $\tau_\phi(P)$ agrees well with the anticipated power law $\tau_\phi \propto P^{-1/5}$ when the field-induced decoherence rate τ_{ac}^{-1} is large compared to the intrinsic decoherence rate τ_o^{-1} , measured in the absence of external fields. As theoretically expected, we observe a decline in field-induced decoherence when $\tau_{ac}^{-1} \leq \tau_o^{-1}$. The frequency dependence of τ_ϕ shows a minimum in the oscillation amplitude at a characteristic frequency $\omega_{ac} \simeq 1/\tau_o$, where τ_o is evaluated from the oscillation amplitude using the standard mesoscopic theory. Both the suppression in the oscillation amplitude and the concomitant change in conductivity allow a direct measurement of the intrinsic decoherence time scale.

DOI: 10.1103/PhysRevB.77.121102

PACS number(s): 73.23.-b, 03.65.Yz, 73.43.Qt

The decoherence time τ_ϕ , the time over which an electron retains its phase information, is of fundamental importance in condensed matter physics.¹ Quantum interference effects such as weak localization (WL), universal conductance fluctuations (UCFs), and Aharonov-Bohm (AB) oscillations in mesoscopic metal samples are characterized by the decoherence time and are limited by decoherence mechanisms such as electron-electron interactions and magnetic impurity spins at temperatures below 1 K. Since intrinsic decoherence mechanisms and their low temperature dependence explore the ground state of the many-body metallic system,^{1,2} precise determination of τ_ϕ is fundamentally important.

In spite of its obvious importance, however, a direct measurement of τ_ϕ in mesoscopic normal metal samples is yet to be reported. Instead, τ_ϕ is obtained as a fit parameter using standard models for quantum corrections to the electrical conductivity, such as WL, UCF, and AB effects. There are several problems in determining τ_ϕ in this way. First, a proper calculation of the decoherence rate due to the coupling to environmental degrees of freedom is usually not contained in a single self-consistent framework except for weak localization.³ Second, the phenomenological introduction of suppression of quantum corrections with temperature (thermal averaging) or decoherence is usually done in an *ad hoc* manner by the inclusion of exponential and multiplicative suppression factors. Lastly, uncertainties in the input parameters, such as sample length, or in the definitions of quantities, such as thermal diffusion length, lead to lack of precision in defining decoherence time⁴⁻⁷ relevant to the experiments. Therefore, a direct measurement of τ_ϕ independent of the specific model of quantum corrections could help shed more light on decoherence mechanisms.

In their pioneering work, Altshuler *et al.*⁸ have shown that electric fields of power P can cause significant decoherence in metal wires as long as τ_{ac}^{-1} , the decoherence rate due to the external high-frequency (hf) electric field, is large compared to the intrinsic decoherence rate τ_o^{-1} , defined in the absence of the external electric field. In this limit, the total decoherence rate $\tau_\phi^{-1} = \tau_o^{-1} + \tau_{ac}^{-1}$ leads to $\tau_\phi \simeq \tau_{ac}$, where $\tau_{ac} \propto P^{-1/5}$. If $\tau_o^{-1} > \tau_{ac}^{-1}$, a decrease in the field-induced decoherence efficiency is expected, and $\tau_\phi \simeq \tau_o$ should be recovered. The

authors also suggest that maximum decoherence occurs for frequencies around $\omega \simeq \tau_\phi^{-1}$ when $\tau_{ac} \ll \tau_o$. By assuming that decoherence mechanisms are the same in a ring geometry, a direct measurement of τ_ϕ may be possible by studying the frequency dependence of the decoherence time $\tau_\phi(\omega)$.

In particular, for the frequency and power dependence of τ_ϕ , the study of AB oscillation amplitude is most suitable as small changes in input parameters can cause significant changes in τ_ϕ due to the exponential dependence of the AB oscillations on τ_ϕ . In comparison, weak localization and conductance fluctuation depend only weakly on τ_ϕ .⁵ Previous high-frequency studies have mostly focused on weak localization effects.¹⁰⁻¹³ In studies of the AB effect under high power, high-frequency fields, Bartolo *et al.*¹⁴ have observed a decline in the oscillation amplitude. In a different approach, Pieper and Price⁶ have attempted to observe strong decoherence by measuring AB oscillations with a high-frequency current itself.

The AB effect in phase coherent, normal metal rings of length L , threaded by a vector potential \vec{A} , was first observed by Webb *et al.*¹⁵ They measured small oscillations in the magnetoresistance of a mesoscopic gold ring with a period of h/e , the flux quantum. These oscillations arise from self-interference of single electrons¹⁶ passing through the ring that acquire a phase due to the vector potential, $(e/\hbar) \int \vec{A} \cdot d\vec{l}$. The amplitude ΔG_{AB} of the AB oscillations in the electrical conductivity or resistance ($\Delta R_{AB} = -R^2 \Delta G_{AB}$) is on the order of the quantum conductance e^2/h . It is reduced due to finite decoherence length $L_\phi = \sqrt{D\tau_\phi}$ and finite temperature T so that

TABLE I. Relevant sample characteristics at $T=0.31$ K. (Errors for τ_o and τ_o^{-1} are obtained from FFT background.)

	Width (nm)	R (Ω)	ΔR_o^a (m Ω)	D_{diff} (m ² /s)	τ_o (ns)	L_ϕ^a (μm)	τ_o^{-1} (MHz)
Ring 1	48.0	28.40	1.82	0.009	2.86 ± 0.13	5.16	350 ± 16
Ring 2	51.1	11.15	0.51	0.022	2.01 ± 0.14	6.69	498 ± 33

^aWithout external field.

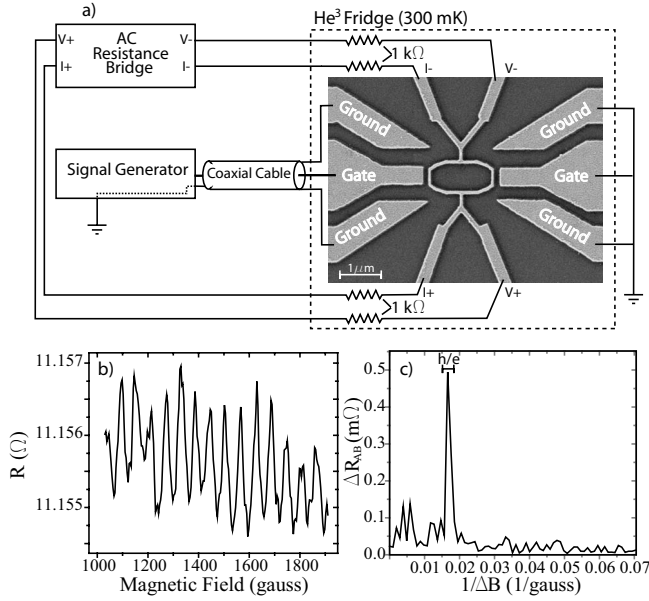


FIG. 1. (a) Schematic of the experimental setup. The resistance of the ring is measured with a standard four-probe, ac resistance bridge technique, while the external field is applied within 100 nm of the gate via coaxial cables and coplanar waveguides. (b) Unperturbed response of the magnetoresistance of ring 2, showing AB oscillations as expected. (c) FFT of the AB oscillations is used to determine the amplitude ΔR_{AB} of the oscillations.

$$\Delta R_{AB} \approx C \frac{e^2 R^2}{h} \left(\frac{L_T}{L} \right) \sqrt{\frac{L_\phi}{L}} e^{-L/L_\phi}, \quad (1)$$

where $L_T = \sqrt{\hbar D / k_B T}$ is the thermal diffusion length, D is the diffusion constant, R is the resistance of the ring, and C is a constant of order unity.¹⁷ The factor $\sqrt{L_\phi / L}$ in Eq. (1) only applies when $L_\phi < L$. Hence, the equation above can be used to obtain τ_ϕ from the AB oscillation amplitude ΔR_{AB} . Yet,

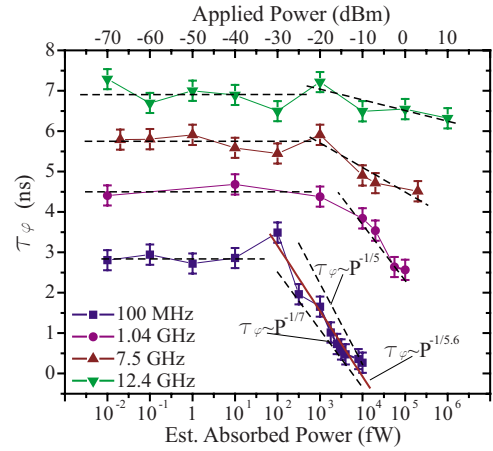


FIG. 2. (Color online) τ_ϕ as a function of power absorbed by ring 1. The red solid line is the fitted power law $\tau_\phi \propto P^{-1/(5.6 \pm 0.5)}$; the dotted lines serve as guide to the eye. All plots have been adjusted for lossy cables and wire bonds. Estimated absorbed power values are obtained from detailed analysis and measurement of transmission coefficients between the ring and gates. (1.04, 7.5, and 12.4 GHz plots are offset for clarity by 2.3, 4, and 6 ns, respectively.)

multiple definitions used for L and L_T ,⁴⁻⁷ as well as significant uncertainties on sample dimensions, constants, and other input parameters, limit the resolution of τ_o^{-1} to an order of magnitude. Even under ideal conditions for given definitions, $C=1$, and minimal uncertainties in input parameters (1 nm resolution in sample dimensions, and 1% error on all other input parameters), τ_o^{-1} as obtained by Eq. (1) can still vary by more than 400 MHz. This lack of precision causes problems for understanding decoherence mechanisms and for numerical comparison between experiments and theory, which could be avoided with a direct measurement of τ_ϕ .

Here, in this Rapid Communication, we study the frequency and power dependence of the field-induced coher-

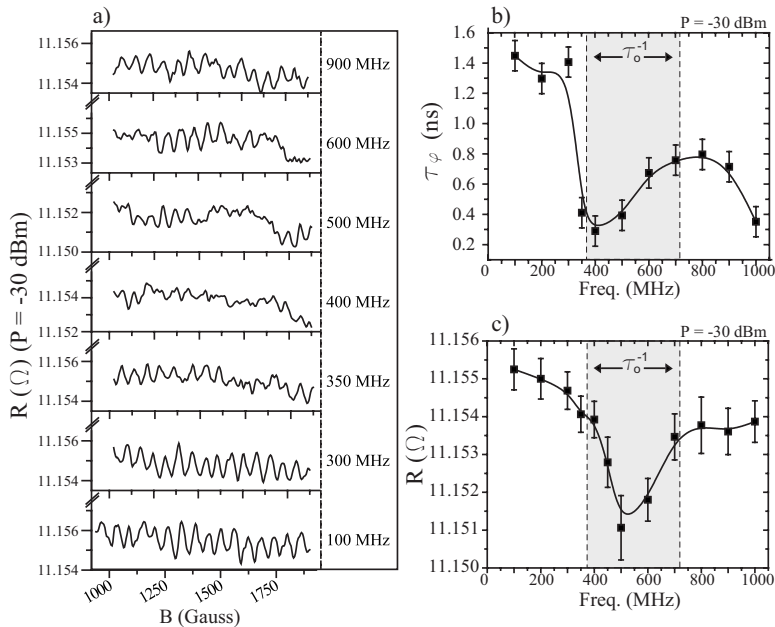


FIG. 3. The lines connecting the data points in (b) and (c) serve as guide to the eye and the shaded regions designate the range of values for τ_o^{-1} under ideal conditions, as described in the text. Data were obtained by measuring ring 2. (a) AB oscillations for different perturbation frequencies at $P = -30$ dBm. Strong oscillations at 100 MHz disappear almost completely at 400 MHz and re-emerge at 900 MHz. (b) $\tau_\phi(\omega)$ extracted from Eq. (1). At $\omega_{ac} \approx \tau_o^{-1}$, a dip is observed. (c) $R(\omega)$ as a function of perturbation frequency. At $\omega_{ac} \approx \tau_o^{-1}$, $R(\omega)$ has a minimum.

ence time τ_{ac} in an attempt to directly identify the relevant time scale for decoherence. We find that the power dependence of τ_ϕ [extracted from Eq. (1)] agrees well with the anticipated power law $\tau_\phi \sim P^{-1/5}$ when $\tau_{ac}^{-1} > \tau_o^{-1}$, and that the field-induced decoherence efficiency declines when $\tau_{ac}^{-1} \leq \tau_o^{-1}$.⁸ We also observe strong decoherence at a specific frequency of $\omega_{ac} \approx \tau_o^{-1}$ along with a concomitant dip in the resistivity at the same frequency. The predicted power dependencies of ω_{ac} was not observed. We suggest that the location of these minima in frequency can be used as a direct measurement of the intrinsic decoherence time τ_o .

The two mesoscopic rings, data from which are reported here, are fabricated using standard e-beam lithography and thermal evaporation of $t=30$ nm thick, ultrapure (99.9999%) silver (Ag) on a SiO₂ substrate. Both rings enclose an area of $A=0.8 \mu\text{m}^2$, with a circumference of $L=3.9 \mu\text{m}$ and gate-to-gate separation of $g \approx 1.6 \mu\text{m}$. Other sample characteristics are summarized in Table I. Ring 1 was used for the power dependence and ring 2 for the frequency dependence data. Similar trends were observed in other ring samples studied in the experiment.

The experimental setup is depicted in Fig. 1(a). The sample is mounted on a specially designed sample stage, attached to the mixing chamber of a He³ cryostat at 300 mK. Resistance is measured via low-frequency twisted pairs with 1 k Ω resistors at 15.9 Hz using a standard four-probe, ac resistance bridge technique, while a hf electromagnetic field (100 MHz–12.4 GHz) is applied in-plane to perturb the ring locally via the left gate. The hf field is guided within $d \approx 100$ nm of the ring utilizing 50 Ω impedance coaxial cables and $\sim 77 \Omega$ impedance microfabricated coplanar waveguides, as measured by time domain reflectometry.

As shown in Fig. 1(b), a typical unperturbed magnetoresistance measurement exhibits AB oscillations with the expected periodicity of $B = \frac{h}{eA} \approx 5.2$ mT. The AB oscillation amplitude ΔR_{AB} is obtained from the fast Fourier transform (FFT) of the magnetoresistance, as shown in Fig. 1(c). The corresponding unperturbed decoherence time and length scales, as determined by Eq. (1), are given in Table I.

According to Ref. 8, τ_{ac} depends on the external field frequency and power. For the rings studied here, the condition $\tau_{ac}^{-1} \geq \tau_o^{-1}$ is satisfied at 1 GHz for applied powers above $P=-30$ dBm, at 7.5 GHz for applied powers above $P=-14$ dBm, and at 12.4 GHz for applied powers above $P=-9$ dBm. Therefore, as a function of power, demonstrated in Fig. 2, we expect $\tau_\phi(P) \propto P^{-1/5}$ for 100 MHz, whereas for frequencies above 1 GHz, a decline in field-induced decoherence efficiency is expected.

This is indeed the case as illustrated in Fig. 2. Each point in Fig. 2 represents τ_ϕ obtained from the FFT of a 3 h magnetoresistance sweep. The error bars for all figures are obtained from the corresponding FFT background. For the 100 MHz data, where $\tau_{ac}^{-1} \geq \tau_o^{-1}$, the red solid line represents the fitted power law $\tau_\phi \propto P^{-1/(5.61 \pm 0.5)}$. The dotted lines for the other frequencies in Fig. 2 (above 1 GHz), where $\tau_{ac}^{-1} \leq \tau_o^{-1}$, represent guides to the eye to point out the anticipated decline in field-induced decoherence efficiency.

Figure 3(a) shows the magnetoresistance in the presence of hf fields for various frequencies at an applied power of -30 dBm. Following the sweeps from 100 to 900 MHz, we

observe two trends. First, there is a minimum in τ_ϕ around 500 MHz, well within the range of theoretically predicted values for τ_o^{-1} under ideal conditions as described above. Second, the overall resistance of the ring, $R(\omega)$, reflects this behavior in that it has a dip around τ_o^{-1} as well. This effect is about four times bigger than the AB amplitude. These two trends are singled out and depicted in Figs. 3(b) and 3(c), respectively.

The data sets indicate that both minima are due to more efficient decoherence at a characteristic frequency of $\omega_{ac} \approx \tau_o^{-1}$. Maximum decoherence at $\omega_{ac} \approx \tau_o^{-1}$ for various powers is depicted in Fig. 4. The precision in the location of the minima suggests that it can be used for direct measurement

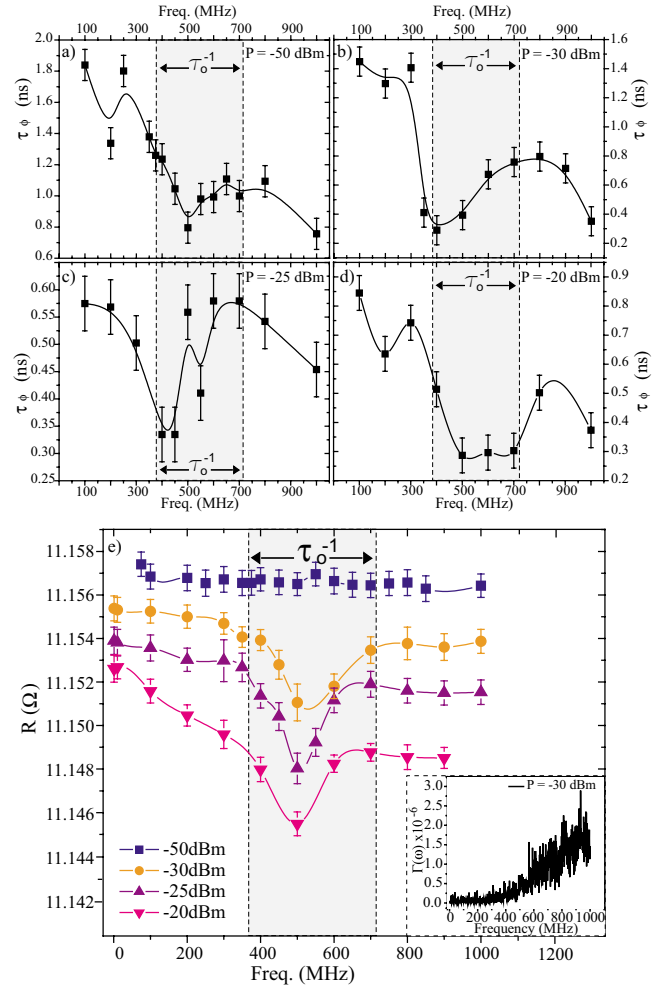


FIG. 4. (Color online) The lines through the data points serve as guide to the eye and the shaded regions demonstrate the uncertainty in τ_o^{-1} under ideal conditions, as described in the text. (a) $\tau_\phi(\omega)$ for ring 2 is depicted as for applied powers of -50 dBm. (b) $\tau_\phi(\omega)$ at -30 dBm. A sharp drop in τ_ϕ is evident at $\omega_{ac} \approx \tau_o^{-1}$. (c) $\tau_\phi(\omega)$ at -25 dBm. (d) At -20 dBm, the system is strongly perturbed but again exhibits a minimum at $\omega_{ac} \approx \tau_o^{-1}$. (e) Composite graph of $R(\omega)$ of the ring for several different powers (-50 , -25 , and -20 dBm data are offset for clarity by 1, -1 , and -2 m Ω , respectively). The inset demonstrates the frequency dependence of gate-to-gate transmission coefficient $\Gamma(\omega)$. All graphs show lower values of $\tau_\phi(\omega)$ for higher frequencies, which can be attributed to the monotonic increase in $\Gamma(\omega)$.

of the intrinsic decoherence time scale. While the determination of τ_o^{-1} from Eq. (1) is rather imprecise (± 170 MHz) even under ideal conditions, it can be measured directly within ± 25 MHz, as can be seen in Fig. 4(e).

Although a nonmonotonic dependence like the minimum in $R(\omega)$ could potentially arise due to electron-electron interaction, corrections arising from diffusion diagrams are not expected to change at high frequencies. In any case, there are no existing calculations to enable a direct numerical comparison.

In order to avoid electron heating, observed here for low-frequency measurement powers of above 20 pW, the power level is kept at $P_{dc} \approx 10$ pW. We have also performed detailed measurement and analysis following Refs. 9, 11, 18, and 19, and we find that the minimum cooling power P_{diff} , provided by the out-diffusion of hot electrons into cooler pads, is larger than the maximum microwave heating power P_{ac} due to the power absorbed by the electrons.

The power absorbed by the ring due to the hf signals arises from the open-ended coplanar waveguide, substrate surface waves, and capacitive coupling between the gates with the ring in the middle.^{20–22} Rigorous analysis shows that the contributions from the first two mechanisms are small ($\sim 10^{-14}$ W) compared to the contribution due to capacitive coupling. Therefore, to estimate the power absorbed by the ring, we have measured the frequency dependent gate-to-gate transmission coefficients $\Gamma(\omega)$ of hf signals released from the top of the He³ refrigerator for several identical rings [see inset of Fig. 4(e)]. Using the maximum transmission coefficient $\Gamma_{\max} = 7 \times 10^{-5}$ and the maximum applied voltage waves of $V_{\max} = 22 \times 10^{-3}$ V, we estimated the upper limit of the power absorbed by the ring to be $[P_{ac}]_{\max} = V_{\max}^2 \Gamma_{\max}^2 L^2 / g^2 R \approx 2 \times 10^{-12}$ W. While $\Gamma(\omega)$ monotonically increases with ω , and thus explains the overall decline in τ_ϕ in Fig. 3(b) for higher frequencies, it does not explain the nonmonotonic behavior at $\omega \approx \tau_o^{-1}$.

The cooling power due to the out-diffusion of hot electrons into cooler current leads depends on the temperature gradient between the hot and cold electrons. By assuming the

smallest significant temperature gradient of $\Delta T_{\min} = 50$ mK, the minimum cooling power can be calculated:⁹ $[P_{diff}]_{\min} = (2\pi k_B T / e)^2 (T \Delta T_{\min} / R) \approx 4 \times 10^{-11}$ W. Since $[P_{ac}]_{\max} < [P_{diff}]_{\min}$, Joule heating can be neglected.

However, P_{ac} is large enough to cause decoherence. According to Refs. 9 and 11, the electric field amplitude E_{ac} required to cause strong decoherence for hf signals in the optimal frequency range of $\omega \tau_\phi \approx 1$ can be estimated as $eE_{ac} L_\phi \sim \hbar / \tau_\phi$. Therefore, the minimum power required to cause strong decoherence is $P_\phi = (E_{ac} L)^2 / R \approx 3 \times 10^{-15}$ W. This is in good agreement with our data, as strong decoherence is observed for applied powers from -20 to -30 dBm, representing a power range experienced by the ring between 0.13 and 1.3 pW according to $[P_{ac}] = V^2 \Gamma^2 L^2 / g^2 R$, but only weak decoherence is found for -50 dBm, representing an estimated maximum absorbed power of 1.3 fW [see Fig. 4(e)].

The correlation between the unique dependence of both $\tau_\phi(\omega)$ and the overall resistance $R(\omega)$ cannot be explained by the fact that τ_ϕ depends on R , as the change in R of ~ 4 m Ω is too small to cause a significant change in τ_ϕ . Furthermore, nonmonotonic dependencies, as seen in Figs. 4(a)–4(e), are not expected from Joule heating, the standard electron interaction correction, $\Delta R_{ee} \sim \frac{e^2 L_T R^2}{hL}$,¹ or the photovoltaic effect in mesoscopic metal rings.¹⁴

In conclusion, we have experimentally measured the dependence of Aharonov-Bohm oscillation amplitude in mesoscopic rings on external electromagnetic fields, applied controllably through a local gate. We find that for $\tau_{ac}^{-1} > \tau_o^{-1}$, the power dependence of coherence time agrees fairly well with $\tau_\phi(P) \propto P^{-1/5}$, while for higher frequencies, when $\tau_{ac}^{-1} < \tau_o^{-1}$, the expected decline in decoherence efficiency is observed. At the characteristic frequency $\omega_{ac} \approx 1 / \tau_o$, we observe strong decoherence and a corresponding dip in the resistivity. We suggest that the location of these minima can be used to determine τ_o directly.

This work was supported by the NSF (CCF-0432089).

¹For a recent review, see L. Saminadayar *et al.*, *Physica E* (Amsterdam) **40**, 12 (2007).

²P. Mohanty *et al.*, *Phys. Rev. Lett.* **78**, 3366 (1997).

³D. S. Golubev *et al.*, *Phys. Rev. Lett.* **81**, 1074 (1998).

⁴F. P. Milliken *et al.*, *Phys. Rev. B* **36**, 4465 (1987).

⁵P. Mohanty, *Complexity from Microscopic to Macroscopic Scales: Coherence and Large Deviations*, NATO Advanced Studies Institute, Series: Mathematics, Physics and Chemistry, Part II, Vol. 63 (Kluwer, Dordrecht, 2001).

⁶J. B. Pieper *et al.*, *Phys. Rev. Lett.* **72**, 3586 (1994).

⁷V. Chandrasekhar *et al.*, *Phys. Rev. Lett.* **55**, 1610 (1985).

⁸B. L. Altshuler *et al.*, *Solid State Commun.* **39**, 619 (1981).

⁹B. L. Altshuler *et al.*, *Physica E* (Amsterdam) **3**, 58 (1998).

¹⁰S. Wang *et al.*, *Phys. Rev. Lett.* **59**, 1156 (1987).

¹¹J. Wei *et al.*, *Phys. Rev. Lett.* **96**, 086801 (2006).

¹²A. A. Bykov *et al.*, *J. Phys. C* **21**, L585 (1988).

¹³R. A. Webb *et al.*, in *Quantum Coherence and Decoherence*, edited by Y. A. Ono and K. Fujikawa (North Holland, Amsterdam, 1999), p. 195.

¹⁴R. E. Bartolo *et al.*, *Phys. Rev. B* **55**, 2384 (1997).

¹⁵R. A. Webb *et al.*, *Phys. Rev. Lett.* **54**, 2696 (1985).

¹⁶Y. Aharonov *et al.*, *Phys. Rev.* **115**, 485 (1959).

¹⁷S. Washburn *et al.*, *Adv. Phys.* **35**, 375 (1986).

¹⁸M. Kanskar *et al.*, *Phys. Rev. Lett.* **73**, 2123 (1994).

¹⁹J. Liu *et al.*, *Phys. Rev. B* **43**, 1385 (1991).

²⁰K. Beilenhoff *et al.*, *IEEE MTT-S Int. Microwave Symp. Dig.* **41**, 1534 (1993).

²¹C. Wood *et al.*, *Electron. Lett.* **14**, 121 (1978).

²²J. R. James *et al.*, *Electron. Lett.* **9**, 570 (1973).